Acta Neuropathol (2017) 133:629–644
DOI 10.1007/s00401-017-1677-y

ORIGINAL PAPER

Pan-mutant IDH1 inhibitor BAY 1436032 for effective treatment of *IDH1* mutant astrocytoma in vivo

Stefan Pusch[1,2] · Sonja Krausert[1] · Viktoria Fischer[1,2] · Jörg Balss[1,2] · Martina Ott[3,4] · Daniel Schrimpf[1,2] · David Capper[1,2] · Felix Sahm[1,2] · Jessica Eisel[1] · Ann-Christin Beck[1] · Manfred Jugold[5] · Viktoria Eichwald[5] · Stefan Kaulfuss[6] · Olaf Panknin[6] · Hartmut Rehwinkel[6] · Katja Zimmermann[7] · Roman C. Hillig[6] · Judith Guenther[6] · Luisella Toschi[6] · Roland Neuhaus[6] · Andrea Haegebart[6] · Holger Hess-Stumpp[6] · Markus Bauser[6] · Wolfgang Wick[4,8] · Andreas Unterberg[9] · Christel Herold-Mende[9] · Michael Platten[3,4] · Andreas von Deimling[1,2]

Received: 13 December 2016 / Revised: 16 January 2017 / Accepted: 16 January 2017 / Published online: 25 January 2017

Abstract Mutations in codon 132 of *isocitrate dehydrogenase* (*IDH*) *1* are frequent in diffuse glioma, acute myeloid leukemia, chondrosarcoma and intrahepatic cholangiocarcinoma. These mutations result in a neomorphic enzyme specificity which leads to a dramatic increase of intracellular D-2-hydroxyglutarate (2-HG) in tumor cells. Therefore, mutant IDH1 protein is a highly attractive target for inhibitory drugs. Here, we describe the development and properties of BAY 1436032, a pan-inhibitor of IDH1 protein with different codon 132 mutations. BAY 1436032 strongly reduces 2-HG levels in cells carrying IDH1-R132H, -R132C, -R132G, -R132S and -R132L mutations. Cells not carrying *IDH* mutations were unaffected. BAY 1436032 did not exhibit toxicity in vitro or in vivo. The pharmacokinetic properties of BAY 1436032 allow for oral administration. In two independent experiments, BAY 1436032 has been shown to significantly prolong survival of mice intracerebrally transplanted with human astrocytoma carrying the IDH1R132H mutation. In conclusion, we developed a pan-inhibitor targeting tumors with different IDH1R132 mutations.

Keywords IDH1R132 inhibitor · IDH-mutated glioma · Pharmacology · Mouse xenograft · Therapy · Drug development

Introduction

Isocitrate dehydrogenase (*IDH*)-mutated glioma is a highly attractive brain tumor for targeted treatment. The identification of mutations in codon 132 of *IDH1* in a small fraction of glioblastomas [24] was followed by the detection of these mutations in the majority of astrocytoma and oligodendroglioma [2, 4, 13, 34, 36]. Approximately, 70–80% of all diffuse astrocytomas and of all oligodendrogliomas were shown to harbor such mutations in *IDH1*. This came

Electronic supplementary material The online version of this article (doi:10.1007/s00401-017-1677-y) contains supplementary material, which is available to authorized users.

✉ Andreas von Deimling
andreas.vondeimling@med.uni-heidelberg.de

1 German Consortium of Translational Cancer Research (DKTK), Clinical Cooperation Unit Neuropathology, German Cancer Research Center (DKFZ), Heidelberg, Germany

2 Department of Neuropathology, Institute of Pathology, Ruprecht-Karls-University Heidelberg, Heidelberg, Germany

3 Clinical Cooperation Unit Neuroimmunology and Brain Tumor Immunology, German Cancer Research Center (DKFZ), Heidelberg, Germany

4 Neurology Clinic and National Center for Tumor Diseases (NCT), University Hospital Heidelberg, Heidelberg, Germany

5 Core Facility, Small Animal Imaging Center, German Cancer Research Center (DKFZ), Heidelberg, Germany

6 Drug Discovery, Bayer Pharma AG, Berlin, Germany

7 Drug Discovery, Bayer Pharma AG, Wuppertal, Germany

8 Clinical Cooperation Unit Neurooncology, German Cancer Research Center (DKFZ), Heidelberg, Germany

9 Division of Experimental Neurosurgery, Department of Neurosurgery, University Hospital Heidelberg, Heidelberg, Germany

as a surprise because a metabolic enzyme decarboxylating isocitrate to α-ketoglutarate (αKG) did not belong to the group of prime suspects for a tumor-promoting gene. Screening in related genes detected mutations in *IDH2* in codons 140 and 172. *IDH2* mutations are rare in brain tumors not exceeding 5% of all *IDH* mutations in astrocytoma or oligodendroglioma [12]. However, in a few other tumor entities harboring *IDH* mutations, the proportion of *IDH2* mutations is much higher than in glioma. Roughly, 15% of patients with acute myeloid leukemia (AML) have *IDH* mutations and more than half of these affect *IDH2* [20, 25]. Chondrosarcomas harbor *IDH* mutations in 50% of the cases, and among those approximately 10% exhibited *IDH2* mutations [1]. *IDH1* and *IDH2* mutations are restricted to few codons only. Most common in brain tumors is the IDH1R132H mutation accounting for approximately 90% of all *IDH* mutations. This mutation type is much rarer in chondrosarcoma (~8%) and AML (~3%), in which the IDH1R132C mutation is more prevalent.

The R132H mutation in IDH1 and the R172K mutation in IDH2 affect the same position of the catalytic center of both enzymes. Further, the R140 mutations in IDH2 likewise alter the configuration of this catalytic center of IDH2. In addition, mutations in either *IDH1* or *IDH2* are always heterozygous. This suggested a gain of function mediated by these mutations. Indeed, mutant IDH1 and IDH2 proteins attain a new specificity for αKG, reducing this metabolite to D-2-hydroxyglutarate (2-HG) thereby consuming NADPH [8]. This neomorphic function is thought to be the main trigger for cancer development in all tumor entities with *IDH* mutations (Supp. Figure 1A).

The resulting very high intracellular levels of 2-HG inhibit αKG-dependent dioxygenases, thereby affecting the methylation status of histones and the cellular DNA. This opens the possibility for the development of specific inhibitors with activity only for mutant, but not for wild-type IDH protein.

Another reason rendering specific IDH inhibitors attractive is the clonal distribution of the mutated protein. Analyses on brain tumors with the IDH1R132H mutation-specific antibody H09 revealed that the mutant protein is virtually present in every tumor cell [5]. Further, the expression of mutant protein is observed throughout all tumor grades from diffuse astrocytoma or oligodendroglioma of WHO grades II to their anaplastic counterparts and even in glioblastomas, which have progressed from these lesions. This suggests dependency of these tumors on the presence of mutant IDH protein.

Consequently, inhibitors of mutant IDH1 and IDH2 protein have been developed in several settings and are in clinical testing now. The clinical studies focus on patients with *IDH*-mutated AML and on patients with *IDH*-mutated astrocytoma or oligodendroglioma. The inhibitors developed so far have been shown to be effective in in vitro and in vivo studies in AML models. However, data on the efficacy for brain tumors is sparse and inconsistent [19, 29, 31]. We have developed a novel drug, BAY 1436032, which specifically inhibits the IDH1 mutation mediated reduction of αKG to 2-HG. Here, we provide details of the structure of BAY 1436032 and demonstrate in vitro and in vivo the efficacy of BAY 1436032 for IDH1R132 mutated glioma.

Materials and methods

Chemical reagents

If not stated otherwise, all chemical reagents were purchased from Sigma-Aldrich, St. Louis, USA.

Statistical analysis

The survival analysis was performed with the log-rank test and is shown as the Kaplan–Meier plot. The analysis was performed with Sigma Plot 13.0 (Systat Software GmbH, Erkrath, Germany) and counterchecked by a biostatistician. All other statistical tests were performed as two-sided Student *t* tests in the corresponding software used to create the graphic.

IDH1 mutant generation and cloning

IDH1 mutants were generated using the site-directed mutagenesis and validated as described before (Pusch et al. Acta Neuropath Comm 2014). The pDONR221 clones were used for all further LR reactions into the described destination vectors. LR reactions were performed following the manufacturer's protocol (Invitrogen, Carlsbad, USA).

Protein production

IDH1R132H enzyme: full-length human recombinant IDH1R132H enzyme with a StrepII tag and expressed in *E. coli* was obtained from BAYER Protein Technologies (Bayer, Berlin, Laboratory Stegmann).

IDH1R132C enzyme: full-length human recombinant IDH1R132C enzyme with a StrepII tag and expressed in *E. coli* was obtained from BAYER Protein Technologies (Bayer, Berlin, Laboratory Stegmann).

IDH1wt enzyme: full-length human recombinant IDH1wt enzyme with a flag tag and expressed in Sf9 cells was obtained from Biomol (BPS-71075, Biomol GmbH, Hamburg, Germany).

IDH2wt enzyme: full-length human recombinant IDH2wt enzyme with a His/Nus tag and expressed in *E. coli* cells was obtained from BAYER Protein Technologies (Bayer, Berlin, Laboratory Stegmann).

Protein Data Bank (PDB) deposition

The coordinates and structure factors for the crystal structure of IDH1R132H in complex with compound-1 have been deposited with the PDB. The PDB accession code is 5LGE.

Enzymatic assays

The inhibition of IDH1R132H and IDH1R132C was assessed in luminescent and fluorescent NADPH consumption assays. Mutant IDH1 catalyzes the NADPH-dependent reduction of αKG to 2-HG. NADPH consumption was measured by fluorescent readout.

The biochemical reactions were performed at 32 °C in 384-well plates using the following assay buffer conditions: 50 mM Tris, pH 7.5, 100 mM NaCl, 20 mM $MgCl_2$, 0.05% BSA, 0.01% Brij, 20 µM NADPH and 250 µM αKG. The IDH1R132H enzyme was used in a final concentration of 20 nM and the IDH1R132C enzyme in a final concentration of 5 nM (fluorescent readout). The test compounds were used in a concentration range between 0.002 and 10 µM. The final DMSO concentration was 2.4%. The reaction was incubated and measured in a fluorescent reader for 90 min (Ex 340 nm/Em 465 nm). The decrease in fluorescence is proportional to mIDH1 activity. IC50 values are determined by interpolation from plots of relative fluorescence versus inhibitor concentration.

The inhibition of wild-type IDH1 and IDH2 was assessed in a fluorescent NADPH generation assay. Wild-type IDH catalyzes the oxidative decarboxylation of isocitrate, producing αKG and CO_2 while converting $NADP^+$ to NADPH. The biochemical reactions were performed at 32 °C in 384-well plates using the following assay buffer conditions: 50 mM Tris, pH 8.0, 100 mM NaCl, 5 mM $MgCl_2$, 0.05% BSA, 0.01% Brij, 20 µM NADP and 10 µM isocitrate. The IDH1wt and IDH2wt enzyme were used in a final concentration of 0.5 and 0.025 nM, respectively. The test compounds were used in a concentration range between 0.002 and 10 µM. The final DMSO concentration was 2.4%. The reaction was incubated for 60 min. NADPH generation is measured by fluorescent detection of NADPH (Ex 340 nm/Em 465 nm). The increase in fluorescence is proportional to IDH1/2wt activity. IC50 values are determined by interpolation from plots of relative fluorescence vs inhibitor concentration.

Cell culture

The glioblastoma cell line LN229, human embryonic kidney cell line HEK293 and sarcoma cell line HT1080 were obtained from ATCC and cultured under standard culture conditions (37 °C, 5% CO_2) in DMEM medium with 1% penicillin and streptomycin and 10% fetal calf serum (all obtained from Gibco® Invitrogen, Carlsbad, USA). HT1080 was cultured in MEM instead of DMEM. For the generation of LN229 IDH1R132H overexpressing cells, IDH1R132H in the destination vector pDEST26 (N-terminal 6× His tag) was used. LN229 cells were transfected with IDH1R132H in pDEST26 vector by FuGene®HD (Promega, MD, USA) followed by picking of single cell clones. Single cell clones were selected with 2 mg/ml gentamicin (Invitrogen, Carlsbad, USA). Clones that survived selection were analyzed for their expression of IDH1R132H by western blot. Clone H77 was chosen for experiments, due to its high and stable expression level of IDH1R132H. To generate HEK293 cell lines which express IDH1wt and mutant proteins, we used cDNAs in pMXs-GW-IRES-BsdR transfected with FuGene®HD (Promega, Madison, USA). Cells were subsequently put under selection pressure by adding 4 µg/ml Blasticidin S. As control we used GFP in pMXs-GW-IRES-BsdR.

HCT116/HD104-013, a human colon cancer cell line, harbors an IDH1R132H heterozygous knock-in and was obtained from Horizon Discoveries (Horizon, Waterbeach, UK). HCT116 IDH1R132H cells were maintained in DMEM/F12 with 10% FCS.

NCH551b, a primary patient-derived secondary glioblastoma cell line, features an endogenous IDH1R132H mutation and was obtained from the group of Prof. Christel Herold-Mende. Specifications to NCH551b and the primary tumor are given in the supplements and supplementary Fig. 2. NCH551b cells were maintained in DMEM/F12 (2 mM GlutaMax) with 2% B27 supplement (Gibco® Invitrogen, Carlsbad, USA), 4 ng/ml EGF (human recombinant, PeproTech, Rocky Hill, USA), 4 ng/ml bFGF (human recombinant, PeproTech, Rocky Hill, USA) and 1% Pen/Strep antibiotic (Gibco® Invitrogen, Carlsbad, USA).

All cells were tested for *Mycoplasma* contamination (PCR-Mycoplama Test Kit II; #A8994, Applichem, Darmstadt, Germany) and IDH1R132H expression (with IDH1R132H Antibody; #DIA-H09, DIANOVA Vertriebs-Gesellschaft mbH, Hamburg, Germany) on a monthly basis. Cell line authentication of NCH551b was done at the Leibniz Institute DSMZ-German Collection of Microorganisms and Cell Cultures, one passage before the start of the experiments. The origin of xenograft from the original tumor was confirmed by analyzing the respective copy number profiles (data not shown).

2-HG assay

The 2-HG assay has been described previously [3]. In brief, the probe material was treated with a deproteinization kit (Biovision, Mountain View, CA, USA). Supernatants were then collected and stored at −20 °C. The total enzymatic

reaction volume was 100 µl. Ten milliliters of assay solution was freshly prepared for each 96-well plate subjected to 2-HG assay. The assay solution contained 100 mM HEPES pH 8.0, 100 µM NAD^+ (Applichem, Darmstadt, Germany), 0.1 µg HGDH, 5 µM resazurin (Applichem, Darmstadt, Germany) and 0.01 U/ml diaphorase (0.01 U/ml; MP Biomedical, Irvine, USA). Immediately before use, 25 µl sample volume was added to 75 µl of assay solution and incubated at room temperature for 30 min in black 96-well plates (Thermo Fisher Scientific, Waltham, USA) in the dark. Fluorometric detection was performed in triplicate with 25 µl deproteinized sample being analyzed in each reaction with excitation at 540 ± 10 nm and emission of 610 ± 10 nm (FLUOstar Omega, BMG Labtech, Offenburg, Germany).

In vitro IC50 determination

LN229 IDH1R132H, HT1080, HCT116 IDH1R132H and NCH551b cells were seeded in 96-well plate (Thermo Fisher Scientific, Waltham, USA) at nearly 80% confluence. One day after seeding, cells received BAY 1436032 in a full dose–response curve starting with 10 µM concentration in nine dilution steps (1:3 dilution each) in 0.1% DMSO final concentration. Vehicle control was 0.1% DMSO in complete medium. After 24 h cells and medium were collected for 2-HG extraction.

Cell viability assay

NCH551b patient-derived glioma cell lines were seeded with 4000 cells/well in 96-well plates for suspension cells (Saerstedt AG, Nümbrecht, Germany). For each condition, three wells were used. The cells were treated 1 day after seeding with BAY 1436032 at concentrations of 500 nM and 2.5 µM and DMSO as solvent control. Subsequently, measurements were performed on days 7, 14 and 21 after the first inhibitor treatment. The cells received fresh drug-containing medium after the first 7 and 14 days of treatment. Plates were measured with a microplate reader (FLUOstar Omega, BMG Labtech, Offenburg, Germany) at the indicated time points with CTG3D as described in the manufacturer's protocol.

Sphere treatment and embedding

Treatment experiments for sphere embedding were performed in suspension culture six-well plates (Saerstedt AG, Nümbrecht, Germany) with 150,000 cells/well. Cells were harvested and embedded 7, 14 and 21 days after inhibitor treatment. The cells received fresh drug-containing medium after 7 and 14 days of treatment. For analysis, the cells were centrifuged at 50*g* for 5 min. The supernatant was used for 2-HG detection. The cells were then washed with PBS once, centrifuged again and subsequently fixed in 4% buffered formalin (54 mM NaH_2PO_4, 28 mM Na_2HPO_4) for 2 h at room temperature. The fixed spheres were embedded in 1.5% low gelling agarose gel. The agarose block was subsequently dehydrated and embedded into paraffin with the HistoStar™ Embedding Workstation (Thermo Fisher Scientific, Waltham, USA).

Animal experiments

Animal work for the orthotropic brain tumor model was approved by the governmental authorities (Regierungspraesidium Karlsruhe, Germany) and supervised by institutional animal protection officials in accordance with the US National Institutes of Health guidelines Guide for the Care and Use of Laboratory Animals.

Orthotropic brain tumor model

A total of 2×10^5 NCH551b cells were stereotactically implanted into the brains of 28 (DKFZ) or 36 (Bayer HealthCare) female 7- to 9-week-old BALB/c nude mice (CAnN.Cg-Foxn1nu/Crl; Charles River Laboratories, Wilmington, MA, USA). The implantation was performed 2 mm right of the sagittal suture and 3 mm rostral of the occipital suture in a depth of 3.5 mm. The cells were injected in PBS with a concentration of 1×10^5 cells/µl at a flow rate of 1 µl/min. The cells were allowed to settle for 1 min, before the syringe was removed. BAY 1436032 was dissolved in an ethanol:Kolliphor® HS:water (1:4:5) mixture at a concentration of 15 mg/ml (ethanol absolute from Merck KGaA; #1.00983.2511, Kolliphor® HS from BASF, # 50259817; water, *aqua ad iniectabilia* from B.Braun, #2351744) by stirring and sonification. The pH was adjusted to pH 8.0 with NaOH solution. The treatment started 7 days after implantation dependent on the actual body weight of the mice. The BAY 1436032 solution was administered via gavage. The health status of each mouse was checked daily for abortion criteria. The abortion criteria were the loss of 20% body weight, ataxia, apathy or paralysis. Mice fulfilling any one of these criteria were euthanized directly.

Brain preparation

The brains of the euthanized mice were extracted and fixed in 4% buffered formalin solution (54 mM NaH_2PO_4, 28 mM Na_2HPO_4) at 4 °C overnight. Subsequently, brains were cut into 2 mm slices, dehydrated and embedded in paraffin with a HistoStar™ Embedding Workstation (Thermo Fisher Scientific, Waltham, USA).

Specimen for 2-HG determination was cryopreserved by placing in liquid nitrogen and subsequently stored at −80 °C.

Immunohistochemistry

Sections from FFPE blocks were cut into 4 µm with a Microm HM 355 S microtome (Thermo Fisher Scientific, Waltham, USA), dried at 80 °C for 15 min and stained with the corresponding antibody following the Ventana staining procedure (Ventana Medical Systems, Tucson, USA). This included rehydration, which was performed by washing in xylol twice for 5 min, followed by washing in an ethanol dilution row, twice 100% ethanol, once 90% ethanol, once 70% ethanol and finally one washing step in pure water, each for 2 min. Pretreatment with cell conditioner 1 (pH 8) for 30 min at 100 °C, followed by incubation with antibody at 4 °C overnight. Antibody incubation was followed by standard signal amplification including the Ventana amplifier kit, ultraWash, counterstaining with one drop of hematoxylin for 4 min and one drop of bluing reagent for 4 min. For chromogenic detection, ultraView Universal DAB detection kit (Ventana Medical Systems, Tucson, USA) was used. Subsequently, slides were washed in water with a drop of dishwashing detergent and mounted with DEPEX (VWR International, Radnor, PA, USA). In the case of the IDH1R132H-specific antibody, we in addition used the Histofine® MOUSESTAIN KIT (Nichirei Corporation, Chūō, Japan) following the manufacturer's protocol. The antibodies were used as follows: IDH1R132H (1:50; #DIA-H09, DIANOVA Vertriebs-Gesellschaft mbH, Hamburg, Germany), SOX2 (1:1000; #Ab97959, Abcam, Cambridge, UK), S100 (1:500; #Z0311, Dako, Agilent Technologies, Glostrup, Denmark) and GFAP (1:500; #Z0334, Dako, Agilent Technologies, Glostrup, Denmark).

Results

Screening for specific IDH1R132H inhibitors

We developed a biochemical assay for the detection of mutant IDH activity. This assay detects residual NADPH by a luminescent readout assay following a defined incubation period (Supp. Figure 1a). Although *IDH* mutations are heterozygous, our assay employed homodimeric mutant enzyme to select against substances interfering with enzyme dimerization.

A library containing more than 3 million compounds was screened using DMSO as negative control and the reaction without αKG as positive control (Supp. Figure 1b). We validated hits from a first round in a secondary screen and further tested the positive hits from this screen against wild-type IDH1 protein. Our criteria for the final hit list were IC50 concentrations lower than 20 µM for IDH1R132H protein and a 20-fold higher IC50 for wild-type IDH1, or IC50 concentration lower than 1 µM for IDH1R132H protein and a 10-fold higher IC50 for wild-type IDH1. Applying these criteria, we identified 377 compounds with potential for specifically inhibiting IDHR132H mutant protein (Supp. Figure 1c).

Development of inhibitors of mutant IDH1

The hit list contained 377 compounds with inhibitory effect on IDH1R132H mutant protein. These were prioritized based on their structure and organized into 51 chemically distinct clusters. Based on previous experience, we selected four clusters with an IC50 ranging from 0.6 to 17.1 µM for further evaluation and processing. This included chemical modifications of the core structures and substituents and retesting of the modified compounds for their ability to inhibit IDH1R132H and wild-type IDH1 protein function. This approach led to a potent lead compound (Fig. 1a), which, upon a full lead optimization program, resulted in BAY 1436032 (Fig. 1a). BAY 1436032 exhibits an IC50 of 15 nM for mutant IDH1R132H protein and virtually no effect on wild-type IDH1 and the structurally related IDH2 proteins with IC50 of 20 and >100 µM, respectively. Testing of BAY 1436032 for its ability to inhibit recombinant IDH1R132C mutant protein revealed an identical inhibitory effect (IC50 of 15 nM) (Fig. 1b). This came as a surprise because the testing assay was devised for the IDH1R132H mutation. The inhibition due to BAY 1436032 is of competitive nature and can be released by titrating αKG into the reaction (Fig. 1c). Although we were not able to co-crystallize BAY 1436032 with mutant IDH1 protein, we managed to co-crystallize an IDH1R132H homodimer with the chemically related compound-1 from the lead optimization program (Fig. 1a). The crystal structure (Fig. 1d–f; Supp. Table 1) shows that compound-1 does not bind in the active site, but in an allosteric pocket located between the two IDH1R132H molecules of the homodimeric IDH1R132H complex. The benzimidazole scaffold and the aniline nitrogen form two hydrogen bonds to Ser280, while the carboxyl group interacts via a salt bridge with His132 from the R132H mutation (Fig. 1f). The isopropylphenyl and cyclohexyl groups insert into hydrophobic subpockets within the binding cavity, which is almost completely buried and shielded from the solvent. Based on this structure, it is possible to conclude that this inhibitor series acts via an allosteric mechanism of inhibition. In a next step we tested BAY 1436032 for off-target effects on kinases, αKG-dependent enzymes or other vital targets such as hERG. We did not detect any relevant off-target effects, except for angiotensin 2 (AT2) which was inhibited with an IC50 of 4.2 µM (Supp. Figure 3a). Thus, we developed a highly specific and potent inhibitor for IDH1 proteins carrying R132H or R132C mutations.

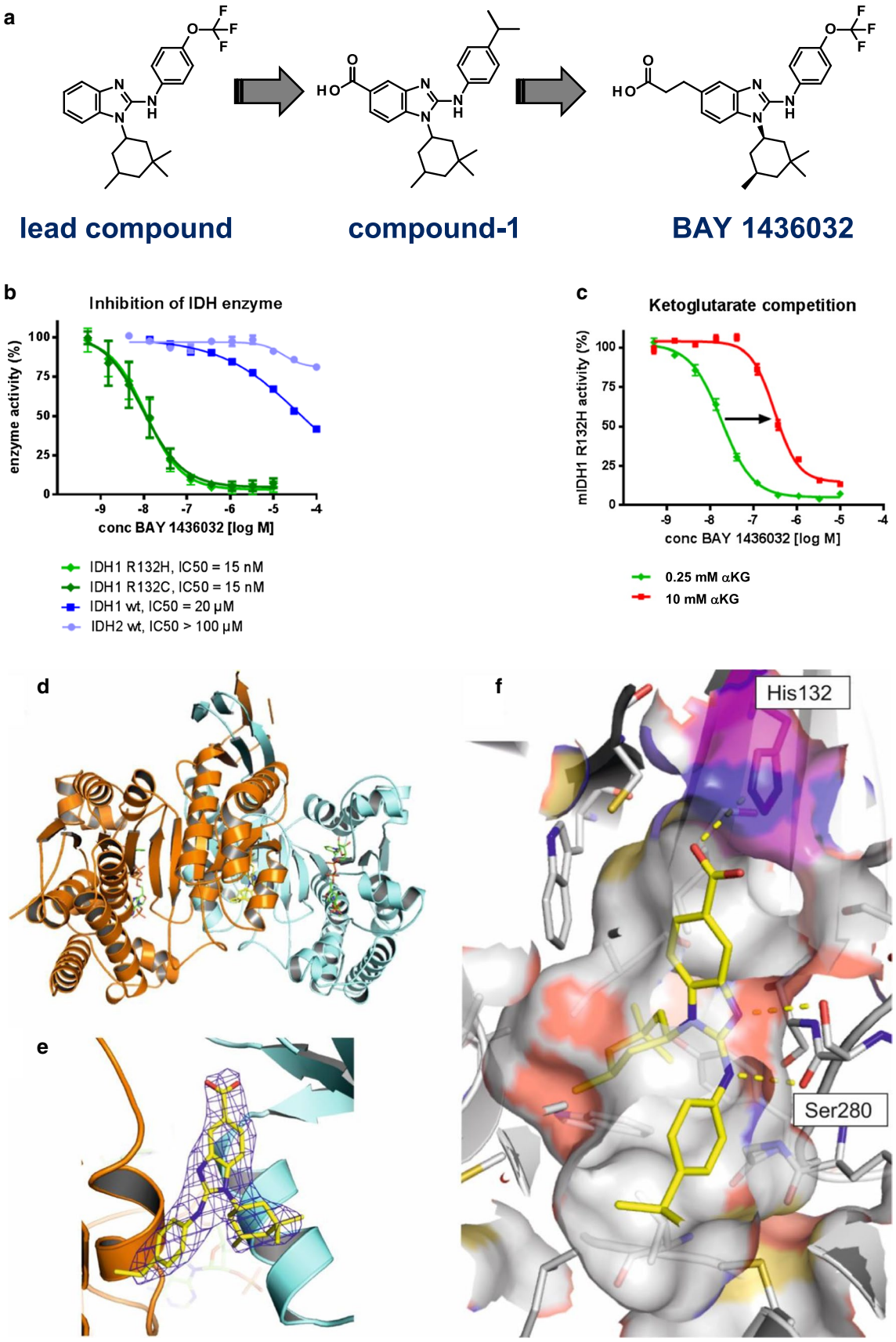
a
lead compound
compound-1
BAY 1436032
b
Inhibition of IDH enzyme
enzyme activity (%)
conc BAY 1436032 [log M]
IDH1 R132H, IC50 = 15 nM
IDH1 R132C, IC50 = 15 nM
IDH1 wt, IC50 = 20 µM
IDH2 wt, IC50 > 100 µM
c
Ketoglutarate competition
mIDH1 R132H activity (%)
conc BAY 1436032 [log M]
0.25 mM αKG
10 mM αKG
d
e
f
His132
Ser280

◂**Fig. 1** BAY 1436032 properties. **a** Chemical structure of lead candidate, co-crystallized compound-1 and BAY 1436032. **b** Biochemical IC50 determination on wild-type IDH1/2 and the mutant proteins IDH1R132H and IDH1R132C (mean ± SD, $n = 3$). **c** Inhibition of IDH1R132H by BAY 1436032 is competitive to αKG (mean ± SD, $n = 3$). **d**–**f** Crystal structure of IDH1R132H in complex with compound-1. **d** One of the two IDH1R132H dimers in the asymmetric unit, shown in ribbon representation (chain A in *orange*, chain B in *blue*). The two NADP molecules and compound-1 are depicted in stick representation (*green* and *yellow* carbon atoms, respectively). **e** 2Fo-Fc electron density map for compound-1 contoured at 1.0σ. **f** View of the allosteric binding site between the two monomers. Polar contacts are indicated by *dotted lines*

Effects of BAY 1436032 on 2-HG production in recombinant and primary human tumor cells

The efficacy of BAY 1436032 for its inhibitory effect on 2-HG production was tested in different recombinant human cell lines. First, we used HEK293T cells ectopically expressing different naturally occurring IDH1 and IDH2 mutant proteins (IDH1 R132H, R132C, R132G, R132S, R132L and R100Q and IDH2 R172K, R172W and R172M). Again, to our surprise, BAY 1436032 not only reduced 2-HG levels in cells with the IDH1R132H or the IDH1R132C mutations, but also in those with the R132G, R132S or R132L mutations with equal efficiency. The inhibitory effect on IDH1 R100Q and IDH2 R172K and R172W were marginal, only around 20%. There was no inhibition of IDH2 R172M (Fig. 2b). Thus, BAY 1436032 exhibited a pan R132-specific inhibition for the five most frequent mutant IDH1 proteins. Next, we used cell lines harboring *IDH1* mutations in a more physiological setting. IDH1R132H was ectopically overexpressed in the human glioma cell line LN229. In addition, we employed the human colon cell line HCT116/HD104-013 carrying a heterozygous knock-in IDH1R132H mutation. BAY 1436032 exhibited an IC50 of 73 nM and 47 nM in LN229 and HCT116/HD104-013, respectively (Fig. 2a, detailed graphs in Supp. Figure 4). We also employed the sarcoma cell line HT1080 carrying a native IDH1R132C mutation, producing high intracellular levels of 2-HG. The IC50 of BAY 1436032 in this cell line was 135 nM (Fig. 2a).

Finally, we determined the IC50 of BAY 1436032 in a primary culture from an IDH1R132H mutant secondary glioblastoma, named NCH551b. This culture is a slowly growing neurosphere culture with comparably low intracellular 2-HG concentrations. We were able to determine an IC50 of 13 nM in NCH551b (Fig. 2a). In conclusion, the pan-IDH1R132 inhibitor BAY 1436032 reduces 2-HG production effectively in engineered and endogenously mutated cells.

BAY 1436032 reduces proliferation and induces differentiation in primary glioma cultures

With a potent inhibitor at hand, we wanted to test if a reduction of 2-HG induces changes in *IDH1* mutant cells. While 2-HG reduction can be detected within hours of inhibition, its effect on cell biology is expected to lag behind. No reduction of cell viability could be detected at days 7 and 14. A significant reduction ($p = 0.012$) of viable cells was first observed after 21 days of incubation with 2.5 µM BAY 1436032, but not with 500 nM (Fig. 2c). However, both concentrations are sufficient to reduce 2-HG levels below 10% of the normal concentration (Supp. Figure 4d). To test for a potential role in differentiation, we assessed the neural stem cell marker SRY-box 2 (SOX2) and the astrocytic differentiation marker glial fibrillary acidic protein (GFAP) with RT-PCR and immunohistochemistry. *SOX2* mRNA levels were significantly reduced (0.2 µM $p = 0.0068$ and 1 µM $p = 0.00052$) after 2 weeks with both treatment conditions (Fig. 2d), but only a concentration of 1 µM of BAY 1436032 reduced *SOX2* expression by 50%. To further confirm this finding, we treated NCH551b neurospheres with 500 nM BAY 1436032 for 3 weeks followed by formalin fixation, paraffin embedding and immunohistochemistry. Control neurospheres treated with solvent only (Fig. 3a) exhibited higher SOX2 levels than BAY 1436032-treated neurospheres (Fig. 3b). The mRNA levels of the differentiation marker *GFAP* increased by a factor of 10 and more (0.2 µM $p = 0.0066$ and 1 µM $p = 0.0088$) in treated cells independent of the concentration of BAY 1436032 used (Fig. 2e). However, the differences regarding *GFAP* expression detected by immunohistochemistry were minute. Control neurospheres treated with solvent only showed very weak GFAP staining with single positive cells (Fig. 3c), whereas treated neurospheres exhibited only slightly stronger GFAP staining with a moderate increase in the number of strong positive cells (Fig. 3d). Thus, the results of both methods pointed toward a differentiation of the treated cells by reduced SOX2 as well as increased GFAP levels. The next step was to assess the additional differentiation markers by immunohistochemistry and to analyze whether BAY 1436032 treatment changes mutant protein expression. BAY 1436032 did not affect protein abundance of the astrocytic differentiation marker solute carrier family 1 member 3 (GLAST), of the oligodendroglial differentiation markers myelin basic protein (MBP), oligodendrocyte lineage transcription factor 2 (OLIG2) and Oligodendrocyte Marker O4. For the neuronal lineage differentiation, we tested beta-III-tubulin (TUBB3), neuronal nuclei (NeuN), microtubule-associated protein 2 (MAP2)

a

mIDH1 tumor cells	Indication	Mutation type	BAY 1436032 IC50 [nM]	basal 2-HG [µM]
LN229 IDH1R132H	glioblastoma (engineered)	IDH1R132H	73	255
HCT116 IDH1R32H	colorectal carcinoma (engineered)	IDH1R132H	47	210
HT1080	sarcoma	IDH1R132C	135	287
NCH551b	secondary glioblastoma	IDH1R132H	13	19

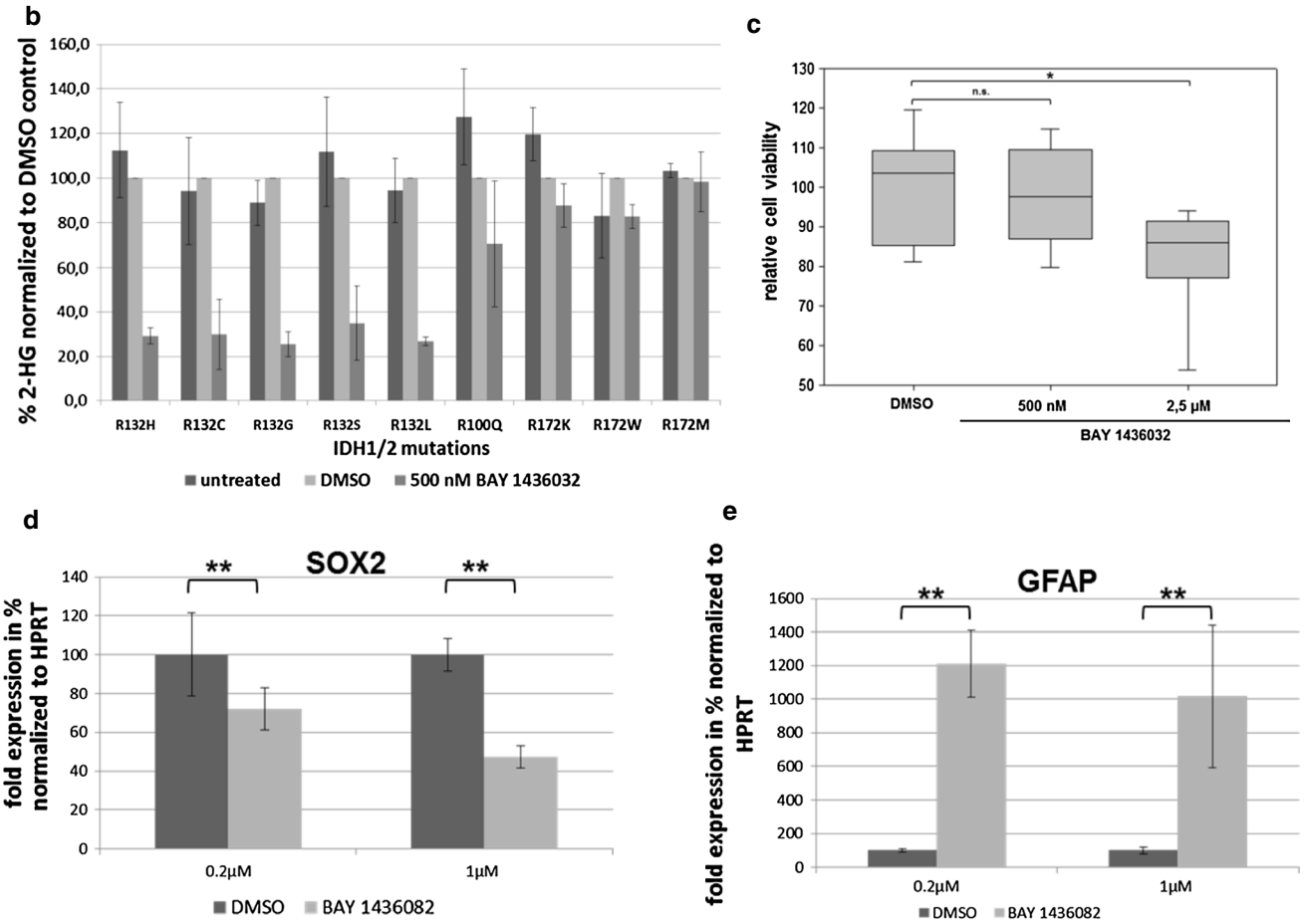

Fig. 2 BAY 1436032 is a pan-R132 inhibitor that reduces proliferation and induces differentiation. **a** In vitro IC50 of BAY 1436032 on engineered and endogenous cell lines determined by intracellular 2-HG measurement. **b** Relative 2-HG levels of untreated and treated HEK293 cells expressing different IDH1 and IDH2 mutations compared to the solvent control DMSO (mean ± SD, $n = 3$). **c** Relative cell viability of NCH551b cells treated for 21 days with 500 nM and 2.5 µM BAY 1436032 compared to solvent control DMSO-treated cells (mean ± SD, $n = 3$). **d** qRT-PCR results of *SOX2* expression normalized on housekeeping gene and compared to DMSO control after 14 days of treatment with 0.2 and 1 µM BAY 1436032 (mean ± SD, $n = 3$). **e** qRT-PCR results of *GFAP* expression normalized on housekeeping gene and compared to DMSO control after 14 days of treatment with 0.2 and 1 µM BAY 1436032 (mean ± SD, $n = 3$). $^*p < 0.05$; $^{**}p < 0.01$

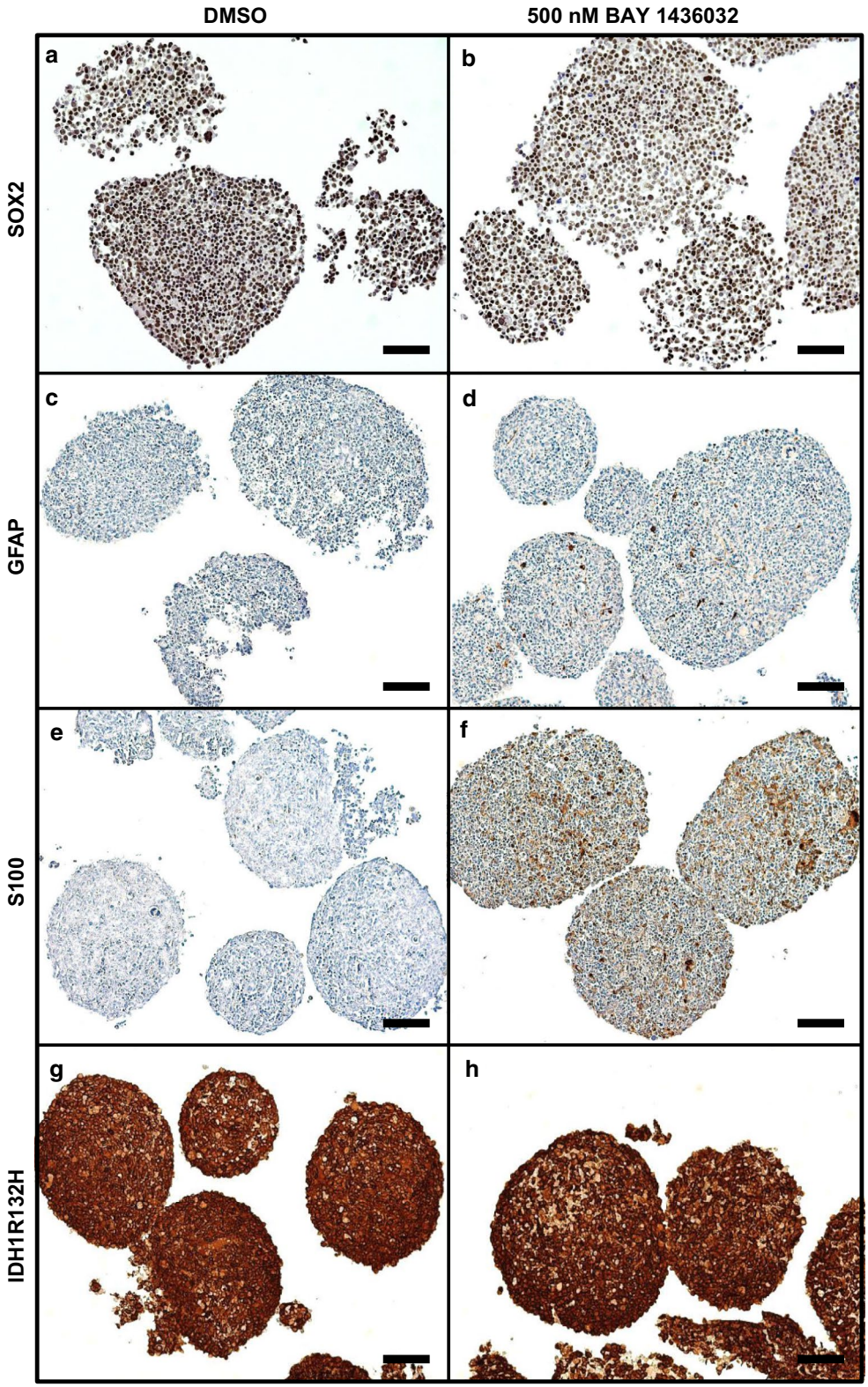

Fig. 3 BAY 1436032 induces differentiation in NCH551b spheres. Images are representative of the findings in triplicate experiments from day 21 after treatment initiation. **a**, **b** SOX2 immunohistochemistry of spheres treated with solvent control (DMSO) (**a**) or 500 nM BAY 1436032 (**b**). **c**, **d** GFAP immunohistochemistry of spheres treated with solvent control (DMSO) (**c**) or 500 nM BAY 1436032 (**d**). **e**, **f** S100 immunohistochemistry of spheres treated with solvent control (DMSO) (**e**) or 500 nM BAY 1436032 (**f**). **g**, **h** IDH1R132H immunohistochemistry of spheres treated with solvent control (DMSO) (**g**) or 500 nM BAY1436032 (**h**). *Scale bar* 100 µm

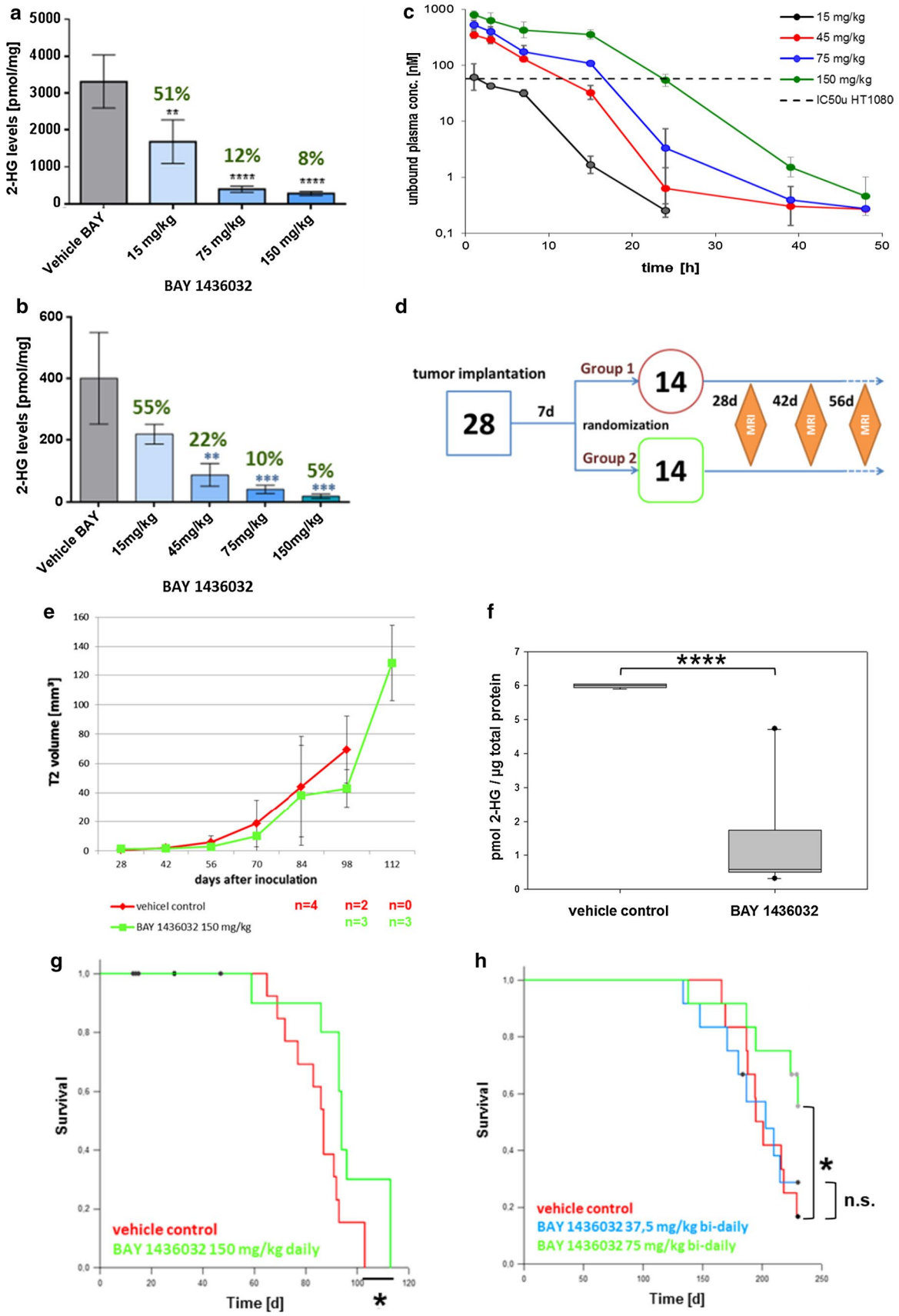
a
2-HG levels [pmol/mg]
5000
4000
3000
2000
1000
0
51%
**
12%
****
8%
****
Vehicle BAY
15 mg/kg
75 mg/kg
150 mg/kg
BAY 1436032
b
2-HG levels [pmol/mg]
600
400
200
0
55%
22%
**
10%
***
5%
***
Vehicle BAY
15mg/kg
45mg/kg
75mg/kg
150mg/kg
BAY 1436032
c
unbound plasma conc. [nM]
1000
100
10
1
0,1
0
10
20
30
40
50
time [h]
15 mg/kg
45 mg/kg
75 mg/kg
150 mg/kg
IC50u HT1080
d
tumor implantation
28
7d
randomization
Group 1
14
Group 2
14
28d
42d
56d
MRI
MRI
MRI
e
T2 volume [mm³]
160
140
120
100
80
60
40
20
0
28
42
56
70
84
98
112
days after inoculation
vehicel control
BAY 1436032 150 mg/kg
n=4
n=2
n=3
n=0
n=3
f
pmol 2-HG / µg total protein
7
6
5
4
3
2
1
0
****
vehicle control
BAY 1436032
g
Survival
1.0
0.8
0.6
0.4
0.2
0.0
0
20
40
60
80
100
120
Time [d]
vehicle control
BAY 1436032 150 mg/kg daily
*
h
Survival
1.0
0.8
0.6
0.4
0.2
0.0
0
50
100
150
200
250
Time [d]
vehicle control
BAY 1436032 37,5 mg/kg bi-daily
BAY 1436032 75 mg/kg bi-daily
*
n.s.

◂**Fig. 4** In vivo efficacy of BAY 1436032 and intracranial xenograft mouse studies with BAY 1436032 treatment. **a** 2-HG levels in subcutaneous LN229 IDH1R132H tumors 15 h after application of different doses of BAY 1436032 (mean ± SD, $n = 3$). **b** 2-HG levels in subcutaneous HT1080 tumors 15 h after application of different doses of BAY 1436032 (mean ± SD, $n = 3$). **c** Unbound concentration–time profiles in plasma of BAY 1436032 after oral administration of 15, 45, 75 and 150 mg/kg (mean ± SD, $n = 3$). *Dashed line* marks the IC50 concentration of HT1080 cells in vitro. **d** Diagram of study design. *Numbers* in the *boxes* depict the number of animals per group. **e** T2 volume increment of NCH551b tumors over time in mm^3 measured in the DKFZ study. Treatment groups are vehicle (*red*) and 150 mg BAY 1436032/kg (*green*) (mean ± SD, $n = 6$ if not otherwise depicted in the graph). **f** 2-HG content of xenograft tumors at the time of death in pmol/µg total protein (*gray box* give upper and lower quartile, the median is depicted as *line* within this *box*, *whiskers* show the full range of data points. $n = 6$ for vehicle control and $n = 14$ for BAY1436032 group). **g** Kaplan–Meier survival analysis of DKFZ mouse study. Treatment once daily with 150 mg BAY 1436032/kg body weight (*green*) or vehicle (*red*). Statistical significance determined with log-rank test. **h** Kaplan–Meier survival analysis of Bayer HealthCare mouse study. Treatment twice daily with 37.5 (*blue*) or 75 mg (*green*) BAY 1436032/kg body weight or vehicle (*red*). Statistical significance determined with log-rank test. *ns* not significant, $^{*}p < 0.05$, $^{**}p < 0.01$, $^{***}p < 0.005$ and $^{****}p < 0.001$

and synaptophysin (SYP). These markers also did not show any alteration in staining intensity upon treatment. Next, we tested additional neural stem cell markers. Vimentin was not affected by BAY 1436032. However, S100 calcium binding protein B (S100B), as a marker for differentiation into a more glial precursor [28], is strongly induced upon treatment (Fig. 3e, f). BAY 1436032 did not affect protein abundance of IDH1R132H (Fig. 3g, h). Immunohistochemical assessment was performed on days 7, 14 and 21 after initiating inhibitor treatment. No evident changes of expression were seen at day 7, but only a weak increase of differentiation markers at day 14 and considerable shift of expression on day 21. The data shown correspond to the expression on day 21 (Fig. 3). In summary, BAY 1436032 reduces proliferation and induces cell differentiation in primary glioma cultures, without altering the expression of mutant IDH1R132H protein.

Pharmacokinetic profile of BAY 1436032 and its effect in vivo

BAY 1436032 revealed low metabolic clearance (CL) in vitro in rat hepatocytes and mice liver microsomes. Its permeability in Caco-2 cells was moderate and in vivo pharmacokinetics (PK) in rats showed low CL and high oral bioavailability (Supp. Figure 3d). We could not determine a maximum tolerated dose (MTD), due to the limited solubility of BAY 1436032 and the absence of toxicity at the highest dose applicable. The encouraging in vitro pharmacological data and the pharmacological profile prompted us to perform experiments in a xenograft animal model. BalbC nude mice with subcutaneously transplanted tumors received a single dose of 15–150 mg/kg BAY 1436032 by gavage. Both, mice with tumors consisting of LN229 cells with ectopic IDH1R132H expression (Fig. 4a) and mice with tumors consisting of HT1080 cells carrying a native IDH1R132C mutation (Fig. 4b), responded 15 h after treatment with decreasing 2-HG levels. In both tumor types, a dose of 15 mg/kg reduced the 2-HG levels by half and the highest tested dose of 150 mg/kg reduced the 2-HG levels below 10% compared to the vehicle controls. To test whether BAY 1436032 is also suitable for brain tumor treatment, we tested brain barrier penetration of the drug in mouse. The maximal intraparenchymal BAY 1436032 concentration amounted to 38% of that in plasma levels. (Supp. Figure 3c). The pharmacokinetic profile (Fig. 4c) suggested that we could work with a single daily dose of 150 mg/kg BAY 1436032. This dose was high enough to ensure unbound plasma levels of BAY 1436032 above the IC50 concentration needed for HT1080 cells, the cells with the highest IC50 of all cells tested in vitro.

BAY 1436032 treatment of intracranial glioma xenografts confers a survival benefit

28 BalbC nude mice were transplanted with human astrocytoma NCH551b line carrying a native IDH1R132H mutation. Cell culture under stem cell conditions and rigorous testing ensured the presence of viable cells carrying the mutation. A series of 14 mice received a daily dose of 150 mg/kg BAY 1436032 (group 1) beginning 7 days after intracranial transplantation of 2×10^5 NCH551b cells. The remaining 14 transplanted mice received vehicle only (group 2) and served as a control (Fig. 4d). Tumor growth of an experimental series at DKFZ was monitored by magnetic resonance imaging (MRI) in six mice of each group on days 28, 42, 56 and 70. On day 84, we could only perform measurements on the four animals remaining alive in the control group. On day 98, only two animals of the control group and three of the treatment group were alive for measurements. On day 112 of the study, only three animals of the treatment group were alive. MRI analysis did not show a significant difference between substance and vehicle-treated groups; there was only a trend for smaller tumor volume in the treated group (Fig. 4e). To test whether BAY 1436032 penetrated the blood brain barrier in sufficient amounts to suppress 2-HG production, we determined the 2-HG concentration in the tumor tissue. The 2-HG concentration in the treated xenografts was significantly lower ($p = 0.00000057$) compared to the untreated controls (Fig. 4f). In addition, survival in the BAY 1436032-treated group was significantly ($p = 0.025$) enhanced (Fig. 4g). We could confirm these findings in a second and independent experimental series conducted at the Bayer Lab. This time

37.5 and 75 mg/kg BAY 1436032 was administered twice daily to 12 animals each while the remaining 12 received vehicle and served as controls. The treatment with a total daily dose of 75 mg/kg failed to show a survival benefit; however, animals treated with a daily total dose of 150 mg/kg BAY 1436032 survived significantly ($p = 0.035$) longer than controls (Fig. 4h). MRI data on this series have not been generated. Thus, oral administration of BAY 1436032 conferred a survival benefit to mice transplanted with *IDH1* mutant tumors.

BAY 1436032 induces differentiation in intracranial xenografts

Next, we examined the effect of BAY 1436032 on the xenografts. We found nuclear SOX2 expression in the tumors of vehicle-treated animals (Fig. 5a), whereas SOX2 expression was reduced by half in tumors of BAY 1436032-treated mice (Fig. 5b). This observation matches the in vitro data. There was no obvious difference in the expression of GFAP in tumors of vehicle- and substance-treated mice in staining intensity or number of stained cells (Fig. 5c, d), but there was a trend toward a more fibrillary phenotype of the GFAP-positive cells in the treated tumors (Fig. 5d). However, the strong induction of S100B, which we could detect in vitro (Fig. 3e, f), cannot be seen in vivo (Fig. 5e, f). The expression of mutant IDH protein assessed by the antibody H09 was not altered by treatment (Fig. 5g, h). This result also recapitulates the in vitro observations.

IDH mutant gliomas are characterized by a hypermethylation phenotype (G-CIMP [22]). To test whether treatment with BAY 1436032 alters G-CIMP, tissue from five treated tumors and six control tumors was subjected to analysis with the human 450K bead array chip (Illumina, San Diego, CA, USA). Unexpectedly, BAY 1436032 had no such effect on DNA methylation and, therefore, treated and control tumors did not form treatment-related cluster groups (Supp. Figure 5a). Detailed analysis revealed neither significant differences in overall genomic (Supp. Figure 5b) or promoter methylation (Supp. Figure 5c) nor on the promoter methylation of SOX2 (Supp. Figure 5d) or GFAP (Supp. Figure 5e).

Discussion

Several IDH inhibitors have been presented since the first report in 2012 [26]. The initial work focused on the potential of inhibitors to reduce 2-HG levels in recombinant cell lines [9, 26] followed by its effect on cells with endogenous mutations in glioma [29] and chondrosarcoma cells [18, 30]. This was followed by the observation that the inhibitors induce differentiation in AML [33]. So far, only two datasets on the effect of IDH inhibitors on intracranial xenografts have been published [19, 31]. One of these studies detected inhibitor-induced differentiation [19], while the other reported no effect of treatment [31]. Nevertheless, several IDH inhibitors are currently under investigation in clinical studies including the drugs AG-221, AG-120 and AG-881 from Agios Pharmaceuticals and IDH305 from Novartis. However, data on the effect of these substances in animals and human patients have not been disclosed so far. We have developed a novel pan IDH1 inhibitor which prolongs survival of mice with human *IDH1*-mutated glioma xenografts.

The lead substance resulting in BAY 1436032 (Fig. 1a) did not exhibit structural similarities to IDH inhibitors previously reported. Although the allosteric inhibition is a common issue of IDH1R132 inhibitors [10, 23, 35, 37], BAY 1436032 shows a different interaction with the mutant IDH1 protein. It is the only one that directly interacts with the mutant residue His132. IC50 of BAY 1436032 was very similar for the five most frequent IDH1 mutations averaging 15 nM (Fig. 2b). The solubility in water was restricted (Supp. Figure 3b); however it could be overcome by adding 10% ethanol to the solvent solution. Full pharmacokinetic profiles have not yet been published for other inhibitors and a comparison of the available data is problematic due to different animal species and drug dosages. We could demonstrate the permeability of the murine blood–brain barrier for BAY 1436032 (Supp. Figure 3c) and show that it is a pan-IDH1R132 mutant inhibitor (Fig. 2b). This has also been stated for AG-881, which in addition also appears to be an inhibitor for mutated IDH2 protein. However, BAY 1436032 exerted only very weak to no inhibition (Fig. 2b) on IDH2R172K and IDH2R172W. We did not test IDH2 R140 mutations, because these appear not to play a role in gliomas, but the efficacy of BAY 1436032 on these mutations is shown in the accompanying paper of Chaturvedi and Herbst et al. [6].

As expected, BAY 1436032 induced differentiation in glioma cells cultured in vitro. The astrocytic marker GFAP was upregulated upon treatment. This matched previous observations on inhibitor-treated cultures. On the other hand, we did not see the also reported effect on the neural stem cell marker nestin [29]. This discrepancy might be due to differing culture conditions. We employed a sphere culture model, whereas adherent cells grown in 1% FCS and 1 µM retinoic acid served as the basis for the previous report. Spheres are known to more closely resemble the pheno- and genotype of the originating tumor [17] and favor a more neural stem cell-like status, thereby possibly impairing differentiation capacity [7, 16]. Nevertheless, upon treatment we could demonstrate a reduction of the stem cell characteristics in our cultures by a decrease in SOX2 expression. We could validate the changes by

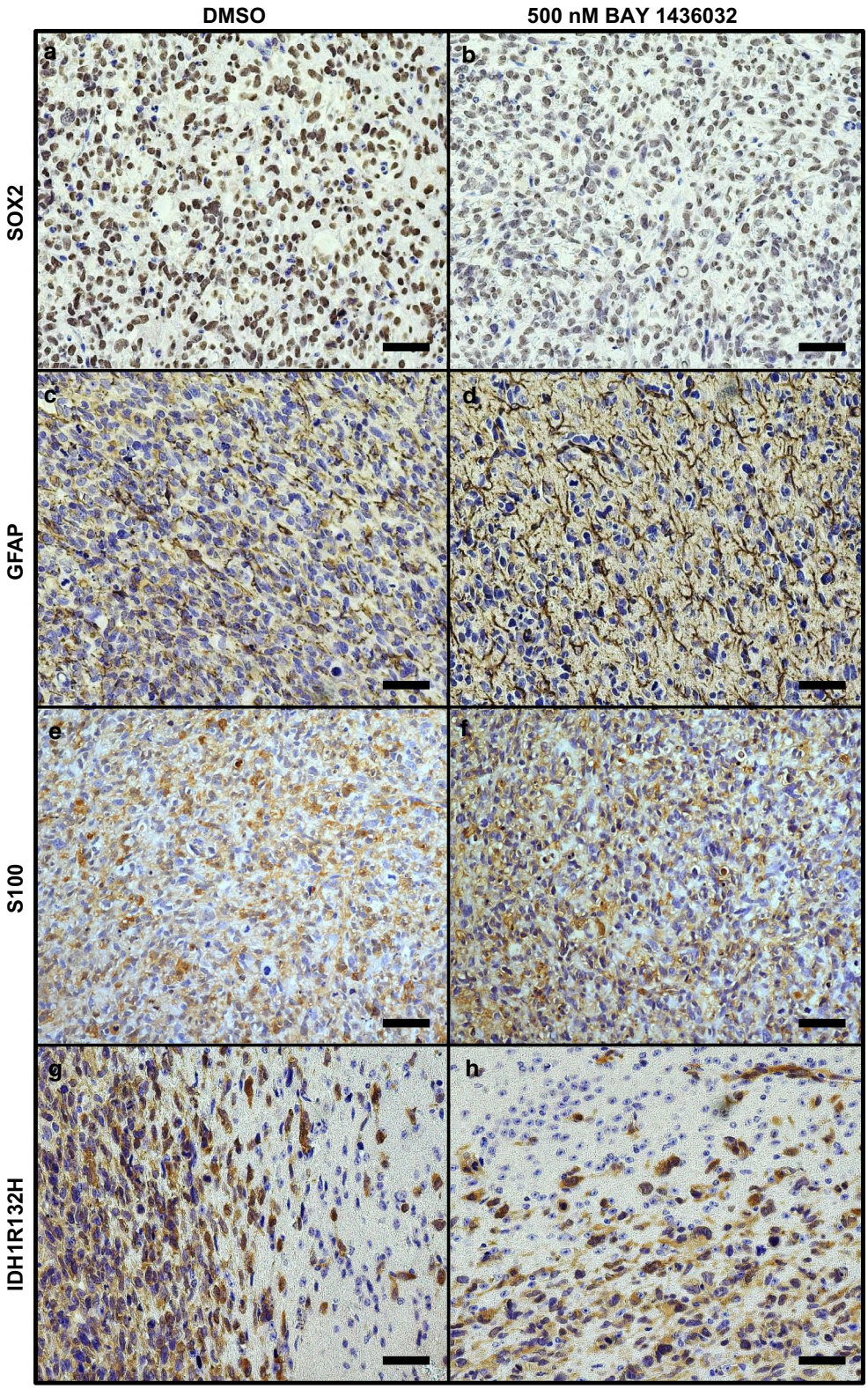

Fig. 5 BAY 1436032 induces differentiation in xenograft tumors. Images are representative for the findings in the respective treatment groups. **a**, **c**, **e**, **g** From a tumor of a vehicle control animal (overall survival 91 days, DKFZ series). **b**, **d**, **f**, **h** From a tumor of a BAY1436032-treated animal (overall survival 93 days, DKFZ series). **a**, **b** SOX2 immunohistochemistry of tumors treated with vehicle control (DMSO) (**a**) or 500 nM BAY 1436032 (**b**). **c**, **d** GFAP immunohistochemistry of tumors treated with vehicle control (DMSO) (**c**) or 500 nM BAY 1436032 (**d**). **e**, **f** S100 immunohistochemistry of tumors treated with vehicle control (DMSO) (**e**) or 500 nM BAY 1436032 (**f**). **g**, **h** IDH1R132H immunohistochemistry of tumors treated with vehicle control (DMSO) (**g**) or 500 nM BAY 1436032 (**h**). *Scale bar* 50 µm

immunohistochemistry on cultured spheres, although the effects are not as pronounced as on mRNA level. In addition, we could also show an increase of S100B abundance, which is a marker for differentiation from a neural stem cell into a more glial precursor [28]. Usually, glial developmental markers [21] are also expressed in glioma cells [11]. However, expression may vary dependent on localization and may be influenced by adjacent cells and environmental conditions such as hypoxia. In addition, the cells of origin in glioma development are still an issue of ongoing debate [11, 14, 16]. Another hallmark of IDH mutant cells is histone methylation, especially the accumulation of trimethylation. Although we know that BAY 1436032 is capable of changing histone methylation (Supp. Figure 6), we could not detect such changes in our sphere culture. Previous work has produced conflicting results. IDH inhibitor effects on methylation of histones range from no changes in intracranial transplants [31] to moderate changes in subcutaneous tumors [29] to strong changes of AQP4 and GFAP promoter-associated histones in differentiated adherent cultures [29].

Our in vivo pharmacokinetic experiments showed that BAY 1436032 can be administered orally. We performed two independent treatment trials on murine orthotropic xenotransplant models in different institutions. In both series, mice receiving the inhibitor survived significantly longer than untreated controls. While we could see a slightly slower tumor growth on MRI scans, the difference between treated and control animals was not significant (Fig. 4e). The time to death was much longer in the set of animals receiving 2 × 75 mg/kg substance than in the set of animals receiving 1 × 150 mg/kg substance per day. We attribute this difference to different husbandry conditions in the respective animal facilities rather than to the different dose scheme of drug administration or implantation procedure of the cells. Differentiation upon treatment was less pronounced in xenotransplants than in sphere cultures (Figs. 3, 5). However, it still may be a major cause for prolonged survival.

To test whether differentiation was an effect of epigenetic reprogramming, we examined DNA from treated and untreated xenotransplants by Infinium Human Methylation450 BeadChip array. There was neither a significant difference in global methylation nor in promoter methylation of GFAP and SOX2 (Supp. Figure 5). Our findings match previous data from subcutaneous xenotransplants [29] and intracranial xenotransplants [31] treated with AGI-5198.

So far, reports on inhibitor-based treatment of *IDH* mutant tumors have forwarded quite inconsistent data. No effect of treatment in other works [31] contrasts with the very encouraging drug-induced effects in our work [19, 29]. Much of these contradictory findings are likely to result from the very different models used. For example, a primary human glioma culture responding with increased proliferation upon IDH inhibitor treatment was derived from a secondary GBM with PNET features which also has *NMYC* amplification [32], the latter probably sufficient to render independency from the driver *IDH1* mutation. This cell line does have some resemblance to our NCH551b with *IDH* mutation and low level *MYC* amplification. However NCH551b also contains a *CDK4* amplification and is *ATRX* mutated, which is typical for diffuse astrocytoma. Thus, the different responses to different inhibitors in different experimental conditions are not surprising. Interestingly, we experienced a proliferative effect with compounds in early development not yet as potent as the clinical compound. This may suggest that a subtle reduction of 2-HG by drugs with reduced efficiency may be beneficiary to *IDH*-mutated cells [27]. Rohle et al. used cells derived from anaplastic oligodendroglioma [29]. These cells were maintained with FCS and retinoic acid representing strong differentiation stimuli. This may explain the difference with our study with respect to nestin expression. A recently presented study is also based on cells derived from *IDH*-mutated GBM [19]. In that subcutaneous xenograft, *GFAP* turned out to be the strongest upregulated gene upon treatment with the Daiichi-Sankyo IDH1 m inhibitor. Interestingly, the same cells intracranially implanted expressed *GFAP* also in untreated condition, supporting the environmental effect on differentiation of cultured glioma. Although culturing tumor cells in spheres tends to conserve the native expression profile [17], they are not unaffected by this method [15]. Thus, current data on IDH inhibitors is inconclusive regarding the effect of mutant IDH inhibition in glioma on tumor growth.

In this study, we describe the development of a highly specific and first potent pan-inhibitor of all IDH1R132 mutations (BAY 1436032). The favorable pharmacological and pharmacokinetic properties of this inhibitor enabled us to perform in vitro and in vivo experiments, in which we can show that this inhibitor is capable of reducing 2-HG levels in engineered and endogenous cell lines in vitro and in vivo. This reduction then leads to changes of neural differentiation markers and results in reduced cell number in a primary culture of a secondary glioblastoma. In this model we can show by two independent studies that administering BAY 1436032 is linked to a significant survival benefit. This could also been shown for the treatment of AML xenograft models with BAY 1436032 [6]. Based on the present work on BAY 1436032, a clinical phase 1 trial (NCT02746081) enrolling solid tumors with IDH1R132 mutations has been initiated.

Acknowledgements We thank Ulrike Hars, Ingo P. Korndoerfer and Ismail Moarefi from Crelux GmbH for excellent structural biology

support, Antje Habel and Viktoria Zeller for histological expertise, Dr. Tim Holland-Letz for biostatistics support and Dr. Ruth Wellenreuther for valuable administrative support.

Compliance with ethical standards

Funding This work was jointly funded by DKFZ and Bayer within their strategic collaboration. Viktoria Fischer is funded by the Bundesministerium für Bildung und Forschung (BMBF; Grant number 031A425A).

Conflict of interest Stefan Pusch, Jörg Balß and Andreas von Deimling are patent holders of "Means and methods for the determination of (D)-2-hydroxyglutarate (D2HG)", the enzymatic 2-HG assay used for 2-HG determination in this manuscript (WO2013127997A1). David Capper, Wolfgang Wick and Andreas von Deimling are patent holders of "Methods for the diagnosis and the prognosis of a brain tumor", the IDH1R132H-specific antibody used in this manuscript (US 8367347 B2). Both patents are under the administrative supervision of the DKFZ technology transfer office. Stefan Kaulfuss, Olaf Panknin, Hartmut Rehwinkel, Katja Zimmermann, Roman C. Hillig, Judith Guenther, Luisella Toschi, Roland Neuhaus, Andrea Haegebart, Holger Hess-Stumpp and Markus Bauser are full-time employees of Bayer Pharma AG and stockholders of Bayer AG share. All other authors declare no potential conflicts of interest.

References

1. Amary MF, Bacsi K, Maggiani F et al (2011) IDH1 and IDH2 mutations are frequent events in central chondrosarcoma and central and periosteal chondromas but not in other mesenchymal tumours. J Pathol 224:334–343
2. Balss J, Meyer J, Mueller W, Korshunov A, Hartmann C, von Deimling A (2008) Analysis of the IDH1 codon 132 mutation in brain tumors. Acta Neuropathol 116:597–602
3. Balss J, Pusch S, Beck A-C et al (2012) Enzymatic assay for quantitative analysis of (D)-2-hydroxyglutarate. Acta Neuropathol 124:883–891
4. Bleeker FE, Lamba S, Leenstra S et al (2009) IDH1 mutations at residue p. R132 (IDH1(R132)) occur frequently in high-grade gliomas but not in other solid tumors. Hum Mutat 30:7–11
5. Capper D, Weißert S, Balss J et al (2010) Characterization of R132H mutation specific IDH1 antibody binding in brain tumors. Brain Pathol 20:245–254
6. Chaturvedi A, Herbst L, Pusch S et al (2017) Pan-mutant-IDH1 inhibitor BAY1436032 is highly effective against human IDH1 mutant acute myeloid leukemia in vivo. Leukemia (**accepted**)
7. Conti L, Cattaneo E (2010) Neural stem cell systems: physiological players or in vitro entities? Nat Rev Neurosci 11:176–187
8. Dang L, White DW, Gross S et al (2009) Cancer-associated IDH1 mutations produce 2-hydroxyglutarate. Nature 462:739–744
9. Davis M, Pragani R, Popovici-Muller J et al (2012) ML309: a potent inhibitor of R132H mutant IDH1 capable of reducing 2-hydroxyglutarate production in U87 MG glioblastoma cells. Probe Reports from the NIH Molecular Libraries Program, City
10. Deng G, Shen J, Yin M et al (2015) Selective inhibition of mutant isocitrate dehydrogenase 1 (IDH1) via disruption of a metal binding network by an allosteric small molecule. J Biol Chem 290:762–774
11. Dirks PB (2010) Brain tumor stem cells: the cancer stem cell hypothesis writ large. Mol Oncol 4:420–430
12. Hartmann C, Meyer J, Balss J et al (2009) Type and frequency of IDH1 and IDH2 mutations are related to astrocytic and oligodendroglial differentiation and age: a study of 1010 diffuse gliomas. Acta Neuropathol 118:469–474
13. Ichimura K, Pearson DM, Kocialkowski S, Backlund LM, Chan R, Jones DT, Collins VP (2009) IDH1 mutations are present in the majority of common adult gliomas but are rare in primary glioblastomas. Neuro Oncol 11:341–347
14. Ilkanizadeh S, Lau J, Huang M, Foster DJ, Wong R, Frantz A, Wang S, Weiss WA, Persson AI (2014) Glial progenitors as targets for transformation in glioma. Adv Cancer Res 121:1–65
15. Laks DR, Crisman TJ, Shih MY et al (2016) Large-scale assessment of the gliomasphere model system. Neuro-oncology 18:1367–1378
16. Ledur PF, Liu C, He H et al (2016) Culture conditions tailored to the cell of origin are critical for maintaining native properties and tumorigenicity of glioma cells. Neuro-oncology 18:1413–1424
17. Lee J, Kotliarova S, Kotliarov Y et al (2006) Tumor stem cells derived from glioblastomas cultured in bFGF and EGF more closely mirror the phenotype and genotype of primary tumors than do serum-cultured cell lines. Cancer Cell 9:391–403
18. Li L, Paz AC, Wilky BA et al (2015) Treatment with a small molecule mutant IDH1 inhibitor suppresses tumorigenic activity and decreases production of the oncometabolite 2-hydroxyglutarate in human chondrosarcoma cells. PLoS One 10:e0133813
19. Machida Y, Ogawara Y, Ichimura K, Matsunaga H, Takahiko S, Araki K, Kitabayashi I (2016) The mutant IDH1 inhibitor prevents growth of glioblastoma with IDH1 mutation in patient-derived xenograft (PDX) model. In: AACR (ed) Proceedings of the 107th annual meeting of the American Association for Cancer Research. AACR, pp Abstract nr 3101
20. Mardis ER, Ding L, Dooling DJ et al (2009) Recurring mutations found by sequencing an acute myeloid leukemia genome. N Engl J Med 361:1058–1066
21. Morrens J, Van Den Broeck W, Kempermann G (2012) Glial cells in adult neurogenesis. Glia 60:159–174
22. Noushmehr H, Weisenberger DJ, Diefes K et al (2010) Identification of a CpG island methylator phenotype that defines a distinct subgroup of glioma. Cancer Cell 17:510–522
23. Okoye-Okafor UC, Bartholdy B, Cartier J et al (2015) New IDH1 mutant inhibitors for treatment of acute myeloid leukemia. Nat Chem Biol 11:878–886
24. Parsons DW, Jones S, Zhang X et al (2008) An integrated genomic analysis of human glioblastoma multiforme. Science 321:1807–1812
25. Paschka P, Schlenk RF, Gaidzik VI et al (2010) IDH1 and IDH2 mutations are frequent genetic alterations in acute myeloid leukemia and confer adverse prognosis in cytogenetically normal acute myeloid leukemia with NPM1 mutation without FLT3 internal tandem duplication. J Clin Oncol 28:3636–3643
26. Popovici-Muller J, Saunders JO, Salituro FG et al (2012) Discovery of the first potent inhibitors of mutant IDH1 that lower tumor 2-HG in vivo. ACS Med Chem Lett 3:850–855
27. Pusch S, Schweizer L, Beck AC, Lehmler JM, Weissert S, Balss J, Miller AK, von Deimling A (2014) D-2-Hydroxyglutarate producing neo-enzymatic activity inversely correlates with frequency of the type of isocitrate dehydrogenase 1 mutations found in glioma. Acta Neuropathol Commun 2:19
28. Raponi E, Agenes F, Delphin C, Assard N, Baudier J, Legraverend C, Deloulme JC (2007) S100B expression defines a state in which GFAP-expressing cells lose their neural stem cell potential and acquire a more mature developmental stage. Glia 55:165–177
29. Rohle D, Popovici-Muller J, Palaskas N et al (2013) An inhibitor of mutant IDH1 delays growth and promotes differentiation of glioma cells. Science 340:626–630

30. Suijker J, Oosting J, Koornneef A et al (2015) Inhibition of mutant IDH1 decreases D-2-HG levels without affecting tumorigenic properties of chondrosarcoma cell lines. Oncotarget 6:12505–12519
31. Tateishi K, Wakimoto H, Iafrate AJ et al (2015) Extreme vulnerability of IDH1 mutant cancers to NAD^+ depletion. Cancer Cell 28:773–784
32. Wakimoto H, Tanaka S, Curry WT et al (2014) Targetable signaling pathway mutations are associated with malignant phenotype in IDH-mutant gliomas. Clin Cancer Res 20:2898–2909
33. Wang F, Travins J, DeLaBarre B et al (2013) Targeted inhibition of mutant IDH2 in leukemia cells induces cellular differentiation. Science 340:622–626
34. Watanabe T, Nobusawa S, Kleihues P, Ohgaki H (2009) IDH1 mutations are early events in the development of astrocytomas and oligodendrogliomas. Am J Pathol 174:653–656
35. Wu F, Jiang H, Zheng B, Kogiso M, Yao Y, Zhou C, Li XN, Song Y (2015) Inhibition of cancer-associated mutant isocitrate dehydrogenases by 2-thiohydantoin compounds. J Med Chem 58:6899–6908
36. Yan H, Parsons DW, Jin G et al (2009) IDH1 and IDH2 mutations in gliomas. N Engl J Med 360:765–773
37. Zheng B, Yao Y, Liu Z, Deng L, Anglin JL, Jiang H, Prasad BV, Song Y (2013) Crystallographic investigation and selective inhibition of mutant isocitrate dehydrogenase. ACS Med Chem Lett 4:542–546